CHEMISTRY OF MATERIALS
Article

Chem. Mater. **2010,** *22,* 5937–5944 5937
DOI:10.1021/cm102047f

Synthesis, Crystal Structure Analysis, and Photoluminescence of Ti^{4+}-Doped $Mg_5SnB_2O_{10}$

Tetsuya Kawano and Hisanori Yamane*

Institute of Multidisciplinary Research for Advanced Materials, Tohoku University, 2-1-1 Katahira, Aoba-ku, Sendai 980-8577, Japan

Received July 23, 2010. Revised Manuscript Received September 20, 2010

Single crystals of magnesium tin oxyborate, $Mg_5SnB_2O_{10}$ ($Mg_5SnO_4(BO_3)_2$), were prepared at 1350 °C in air, using B_2O_3 as a flux. They were colorless and transparent with needlelike or columnar shapes. X-ray diffraction analysis of the single crystals revealed that $Mg_5SnB_2O_{10}$ crystallizes in the triclinic space group $F\bar{1}$ (No. 2) with $Z = 16$, $a = 6.1295(8)$, $b = 18.714(3)$, $c = 24.719(3)$ Å, $\alpha = 90.021(5)°$, $\beta = 90.032(4)°$, $\gamma = 90.041(5)°$, and $V = 2835.4(7)$ Å^3 ($R1 = 0.0168$, $wR2 = 0.0459$, and $S = 1.297$ for all data). The crystal structure of $Mg_5SnB_2O_{10}$ is a ludwigite-type superstructure. Mg and Sn atoms are ordered and coordinated by six O atoms, and the edges of MO_6 (where M = Mg and Sn) octahedra are connected along the a-axis and form zigzag walls. B atoms are in the spaces surrounded by the walls and are coordinated by three O atoms. Polycrystals of titanium(IV)-doped solid solutions, $Mg_5Sn_{1-x}Ti_xB_2O_{10}$ ($0 < x \leq 0.50$), were also prepared by solid state reaction at 1300 °C in air. The refined unit cell volumes decreased with increasing titanium content (x), indicating partial substitution of Ti for Sn atoms. A broad blue emission with a peak wavelength of ~430 nm was observed from the solid solutions under 265-nm ultraviolet excitation. A quantum efficiency of 0.81 was measured at room temperature for $Mg_5Sn_{0.80}Ti_{0.20}B_2O_{10}$.

Introduction

Tetravalent titanium (Ti^{4+}) ions are known as a luminescence center of oxide phosphors,[1] such as $A_2Sn_{1-x}Ti_xO_4$ (where A = Mg,[1−4] Ca,[1,2,5] Sr,[1−3,5] Ba,[1,2,5] and Zn[1,6]), $6.5MgO \cdot 1SnO_2 \cdot 1.5B_2O_3$:Ti,[7] $La_2MgSn_{1-x}Ti_xO_6$,[8] $BaM_{1-x}Ti_xSi_3O_9$ (where M = Sn and Zr),[9,10] $Mg_5Sn_{1-x}Ti_xB_2O_{10}$,[11] $Mg_3Zr_{1-x}Ti_xB_2O_8$,[11] $AZr_{1-x}Ti_x(BO_3)_2$ (A=Ca, Sr, and Ba),[12] $CaSn_{1-x}Ti_x(BO_3)_2$,[13] $CaSn_{1-x}Ti_xSiO_5$,[14] and $Ca_3Sn_{1-x}Ti_xSi_2O_9$.[14] The host compounds of these phophors include Sn^{4+} or Zr^{4+} ions, which can be replaced by Ti^{4+} ions. The Ti^{4+}-doped oxides show broad blue-to-green emission with peak wavelengths of 400−500 nm excited by ultraviolet excitation at 200−300 nm. The emission generally originates from a charge transfer (CT) transition ($^1A_{1g}-{}^3T_{1u}$) between Ti^{4+} and O^{2-} ions in octahedral TiO_6^{8-} complexes.[8,15] Although most of their luminescence properties were reported near the range of ~1970−1990, they have received renewed attention as rare-earth-free phosphors because of recent limited supply and increased demand for rare-earth elements.

Benderskaya et al. reported the luminescence properties of Ti^{4+}-doped magnesium tin borate with a composition of $6.5MgO \cdot 1SnO_2 \cdot 1.5B_2O_3$.[7] Konijnendijk and Blasse subsequently revealed the chemical formula for the compound to be $Mg_5SnB_2O_{10}$ ($Mg_5SnO_4(BO_3)_2$).[11] They also synthesized solid solutions of $Mg_5Sn_{1-x}Ti_xB_2O_{10}$ ($0 < x \leq 1$) and observed broad blue emission with a peak wavelength of ~435 nm under 230 nm excitation for $Mg_5Sn_{0.90}Ti_{0.10}B_2O_{10}$.[11] A quantum efficiency of 0.80 was measured for the solid solutions with compositions of $x = 0.01-0.20$ at room temperature. This value of quantum efficiency is highest among those of Ti^{4+}-doped phosphors. Therefore, the Ti^{4+}-doped $Mg_5SnB_2O_{10}$ has potentials for a phosphor of cold or hot cathode fluorescent lamps. Konijnendijk and Blasse indexed the X-ray diffraction (XRD) reflections of $Mg_5SnB_2O_{10}$ with orthorhombic unit-cell parameters of $a = 19.12$ Å, $b = 12.37$ Å, and $c = 11.44$ Å, and they deemed $Mg_5SnB_2O_{10}$ to be isostructural with orthopinakiolite ($Mg_3Mn_3B_2O_{10}$, orthorhombic, space group *Pnnm* (No. 58), with unit-cell

*Author to whom correspondence should be addressed. Tel./Fax: +81 22 217 5813. E-mail: yamane@tagen.tohoku.ac.jp.

(1) Kröger, F. A. *Some Aspects of the Luminescence of Solids*; Elsevier: Amsterdam, 1948; pp 159−173.
(2) Kotera, Y.; Sekine, T.; Yonemura, M. *Bull. Chem. Soc. Jpn.* **1956**, *29*, 616–619.
(3) Macke, A. J. H. *J. Solid State Chem.* **1976**, *18*, 337–346.
(4) Blasse, G. *Philips Res. Rep.* **1968**, *23*, 344–361.
(5) Yamashita, T.; Ueda, K. *J. Solid State Chem.* **2007**, *180*, 1410–1413.
(6) Blasse, G.; Dalhoeven, G. A. M.; Choisnet, J.; F. Studer, F. *J. Solid State Chem.* **1981**, *39*, 195–198.
(7) Benderskaya, L. P.; Krongauz, V. G.; Khalupovskii, M. D. *J. Appl. Spectrosc.* **1974**, *20*, 238–240.
(8) Macke, A. J. H. *Phys. Stat. Solidi A* **1977**, *39*, 117–123.
(9) Konijnendijk, W. L. *Inorg. Nucl. Chem. Lett.* **1981**, *17*, 129–132.
(10) Iwasaki, K.; Takahashi, Y.; Masai, H.; Fujiwara, T. *Opt. Express* **2009**, *17*, 18054–18062.
(11) Konijnendijk, W. L.; Blasse, G. *Mater. Chem. Phys.* **1985**, *12*, 591–599.
(12) Blasse, G.; Sas, S. J. M.; Smit, W. M. A.; Konijnendijk, W. L. *Mater. Chem. Phys.* **1986**, *14*, 253–258.
(13) Kawano, T.; Yamane, H. *J. Alloys Compd.* **2010**, *490*, 443–447.
(14) Abe, S.; Yamane, H.; Yoshida, H. *Mater. Res. Bull.* **2010**, *45*, 367–372.
(15) Blasse, G. *Struct. Bonding* (*Berlin*) **1980**, *42*, 1–41.

Published on Web 10/12/2010

Table 1. Crystal Data and Refinement Results for $Mg_5SnB_2O_{10}$[a]

chemical formula	$Mg_5SnB_2O_{10}$
formula weight, M_r	421.86 g/mol
temperature, T	25(2) °C
crystal system	triclinic
space group	$F\bar{1}$ (No. 2)
unit-cell dimensions	
a	6.1295(8) Å
b	18.714(3) Å
c	24.719(3) Å
α	90.021(5)°
β	90.032(4)°
γ	90.041(5)°
unit-cell volume, V	2835.4(7) Å^3
Z	16
calculated density, D_{cal}	3.953 Mg/m^3
radiation wavelength, λ	0.71073 Å (Mo Kα)
crystal form, color	needle, colorless
absorption correction	numerical
absorption coefficient, μ	4.104 mm^{-1}
crystal size	0.30 mm × 0.08 mm × 0.07 mm
limiting indices	$-7 \le h \le 7$, $-24 \le k \le 24$, $-32 \le l \le 32$
F_{000}	3200
θ range for data collection	3.3°−27.5°
reflections	
collected	7009
unique	3203
R_{int}	0.0237
data/restraints/parameters	3203/0/207
weight parameters	
a	0.0146
b	15.5346
extinction correction	SHELXL
extinction coefficient	0.00053(2)
twin matrix	[1 0 0, 0 −1 0, 0 0 1]
BASF parameter	0.408
goodness-of-fit on F^2, S	1.297
$R1$, $wR2$ $[I > 2\sigma(I)]$	0.0162, 0.0397
$R1$, $wR2$ (all data)	0.0168, 0.0459
largest diffr. peak and hole, $\Delta\rho$	0.752, −0.956 e/Å^3

[a] $R1 = \sum||F_o| - |F_c||/\sum|F_o|$, and $wR2 = [\sum w(F_o^2 - F_c^2)^2/\sum(wF_o^2)^2]^{1/2}$. $w = 1/[\sigma^2(F_o^2) + (aP)^2 + bP]$, where F_o is the observed structure factor, F_c the calculated structure factor, and σ the standard deviation of F_c^2. The variable P is defined as follows: $P = (F_o^2 + 2F_c^2)/3$. The goodness of fit (S) is defined as follows: $S = [\sum w(F_o^2 - F_c^2)^2/(n-p)]^{1/2}$, where n is the number of reflections and p is the total number of parameters refined.

dimensions of $a = 18.357(4)$ Å, $b = 12.591(2)$ Å, and $c = 6.068(1)$ Å).[16,17] In our preliminary experiments, the XRD pattern of $Mg_5SnB_2O_{10}$ was similar to the patterns of $Mg_3Mn_3B_2O_{10}$ or other oxyborates with a chemical formula of $M^{II}_5M^{IV+}B_2O_{10}$. However, some reflections in the pattern could not be indexed with the reported unit-cell parameters.

Oxyborates with a chemical formula of M_3BO_5 ($M_6B_2O_{10}$) are classified as $M^{II}_2M^{III}BO_5$ or $M^{II}_5M^{IV}B_2O_{10}$. Three structure types of $M^{II}_2M^{III}BO_5$ have been named: orthopinakiolite (orthorhombic, *Pnnm*), ludwigite (orthorhombic, *Pbam*), and pinakiolite (monoclinic, *C*2/*m*).[18] The crystal structures of orthopinakiolite, ludwigite, and pinakiolite are mutually related, as reported by Takéuchi et al.[19] Crystal structures of $M^{II}_5M^{IV}B_2O_{10}$ are basically isostructural with ludwigite. $Ni_5M^{IV}B_2O_{10}$ (where M^{IV} = Ti,[20,21] V,[22] Mn,[22] Ge,[23] and Zr[23]), $Co_5M^{IV}B_2O_{10}$ (M^{IV} = Ti,[20] Mn,[24] and Sn[24]) and $Zn_5MnB_2O_{10}$[25] crystallize in the orthorhombic unit cell with parameters of $a \approx 9$ Å, $b \approx 12$ Å, and $c \approx 3$ Å. $Cu_5SnB_2O_{10}$ (monoclinic, space group $P2_1/c$ (No. 14), $a = 6.3526(7)$ Å, $b = 9.502(1)$ Å, $c = 12.100(9)$ Å, and $\beta = 93.30(3)°$)[26] is a ludwigite-related structure. In the crystal structure of the ludwigite-type $M^{II}_5M^{IV}B_2O_{10}$, as well as $Cu_5SnB_2O_{10}$, M^{IV} atoms occupy mixed sites with a portion of M^{II} atoms, and the mixed sites of M^{II} and M^{IV} atoms are statistically distributed along the *c*-axis (or the *a*-axis for $Cu_5SnB_2O_{10}$). The oxyborates of $Ni_5M^{IV}B_2O_{10}$ (where M^{IV} = Sn[27] and Hf;[28] orthorhombic, space group *Pnma* (No. 62), unit-cell parameters of $a \approx 9$ Å, $b \approx 6$ Å, and $c \approx 12$ Å) have a type of the ludwigite-type superstructure. The Ni and M^{IV} atoms of these oxyborates alternately occupy individual sites along the *b*-axis.

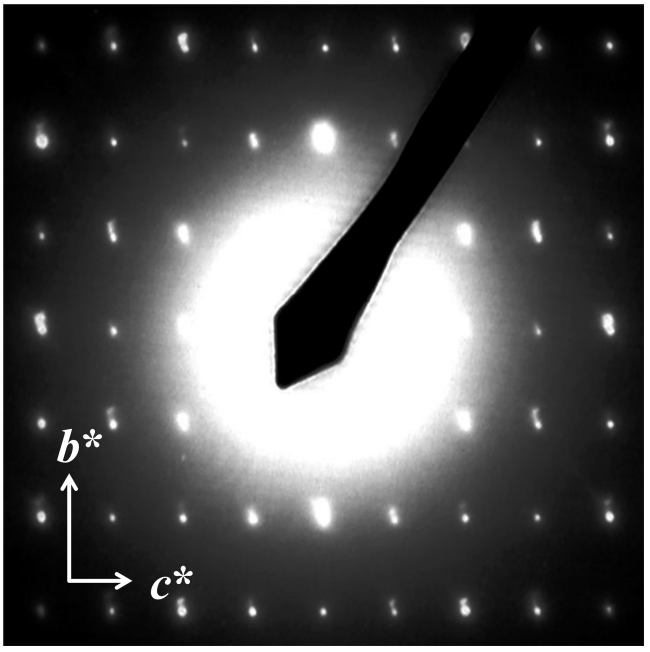

Figure 1. Electron diffraction pattern of $Mg_5SnB_2O_{10}$ taken with the electron beam parallel to the [100] direction.

Although a high quantum efficiency of luminescence was measured for $Mg_5Sn_{1-x}Ti_xB_2O_{10}$ solid solutions as mentioned above, the crystal structure of $Mg_5SnB_2O_{10}$ has not been clarified. In the present study, we synthesized $Mg_5SnB_2O_{10}$ single crystals and analyzed their crystal structure via single-crystal XRD. We also investigated the change of the crystal structures of $Mg_5Sn_{1-x}Ti_xB_2O_{10}$ solid solutions and recharacterized their photoluminescence properties.

(16) Randmets, R. *Arkiv Mineral. Geol.* **1960**, *2*, 551–555.
(17) Takéuchi, Y. *Recent Prog. Nat. Sci. Jpn.* **1978**, *3*, 153–181.
(18) Heller, G. *Top. Curr. Chem.* **1986**, *131*, 39–98.
(19) Takéuchi, Y.; Haga, N.; Kato, T.; Miura, Y. *Can. Mineral.* **1978**, *16*, 475–485.
(20) Stenger, C. G. F.; Verschoor, G. C.; Ijdo, D. J. W. *Mater. Res. Bull.* **1973**, *8*, 1285–1292.
(21) Armbruster, Th.; Lager, G. A. *Acta Crystallogr., Sect. C: Cryst. Struct. Commun.* **1985**, *41*, 1400–1402.
(22) Bluhm, K.; Müller-Buschbaum, Hk. *Z. Anorg. Allg. Chem.* **1989**, *579*, 111–115.
(23) Bluhm, K.; Müller-Buschbaum, Hk. *J. Less-Common Met.* **1989**, *147*, 133–139.
(24) Utzolino, A.; Bluhm, K. *Z. Naturforsch. B* **1996**, *51*, 305–308.
(25) Busche, S.; Bluhm, K. *Z. Naturforsch. B* **1995**, *50*, 1450–1454.
(26) Schaefer, J.; Bluhm, K. *Z. Anorg. Allg. Chem.* **1994**, *620*, 1578–1582.
(27) Bluhm, K.; Müller-Buschbaum, H. *Monatsh. Chem.* **1989**, *120*, 85–89.
(28) Bluhm, K.; Müller-Buschbaum, Hk. *Z. Anorg. Allg. Chem.* **1989**, *575*, 26–30.

Table 2. Atomic Coordinates and Isotropic and Equivalent Isotropic Displacement Parameters, U_{iso}, U_{eq}, for $Mg_5SnB_2O_{10}$ with the $F\bar{1}$ Cell[a]

atom	x	y	z	U_{iso}, U_{eq}[b] (Å^2)
Sn1	0.49986(7)	0.120353(17)	0.057754(17)	0.00367(13)[b]
Sn2	0.99990(7)	0.130103(19)	0.306762(16)	0.00365(13)[b]
Mg1	0.5010(4)	0.13220(11)	0.31030(9)	0.0062(6)[b]
Mg2	0.0001(3)	0.11841(10)	0.05925(8)	0.0052(6)[b]
Mg3	0.7398(3)	0.00003(8)	0.49998(7)	0.0068(5)[b]
Mg4	0.7412(2)	0.25003(7)	0.25006(7)	0.0048(4)[b]
Mg5	0.2448(3)	0.00203(12)	0.14089(8)	0.0052(3)[b]
Mg6	0.7521(3)	0.25181(12)	0.10923(8)	0.0066(3)[b]
Mg7	0.7528(3)	0.24817(12)	0.39078(8)	0.0067(3)[b]
Mg8	0.7543(3)	0.00208(12)	0.14083(8)	0.0048(3)[b]
Mg9	0.4997(2)	0.25630(8)	0.00097(5)	0.0060(4)[b]
Mg10	0.49974(19)	0.00529(7)	0.24995(5)	0.0056(4)[b]
O1	0.9995(6)	0.31184(17)	0.07085(15)	0.0036(6)
O2	0.9985(6)	0.4256(2)	0.02175(13)	0.0067(7)
O3	0.0010(5)	0.0765(2)	0.38234(13)	0.0062(7)
O4	0.4976(5)	0.1748(2)	0.22846(13)	0.0049(7)
O5	0.5002(6)	0.0650(2)	0.17867(14)	0.0096(8)
O6	0.4979(5)	0.1770(2)	0.13177(13)	0.0040(7)
O7	0.5029(5)	0.0723(2)	0.38161(13)	0.0066(7)
O8	0.5010(6)	0.31547(18)	0.07289(14)	0.0046(6)
O9	0.4971(5)	0.4264(2)	0.02145(13)	0.0054(7)
O10	0.9981(5)	0.1754(2)	0.13145(13)	0.0064(7)
O11	0.0001(6)	0.0631(2)	0.17967(14)	0.0066(7)
O12	0.9979(6)	0.1743(2)	0.22801(14)	0.0066(7)
O13	0.2578(5)	0.0521(2)	0.07147(14)	0.0057(7)
O14	0.7458(5)	0.0520(2)	0.07141(13)	0.0036(7)
O15	0.7409(5)	0.1933(2)	0.03871(13)	0.0054(7)
O16	0.2580(5)	0.19318(19)	0.03869(13)	0.0053(7)
O17	0.7570(6)	0.30188(19)	0.17861(16)	0.0060(7)
O18	0.7540(6)	0.19809(19)	0.32153(16)	0.0053(7)
O19	0.7589(5)	0.4434(2)	0.21142(13)	0.0055(7)
O20	0.7600(5)	0.0567(2)	0.28859(13)	0.0066(7)
B1	0.9984(13)	0.3845(3)	0.0692(3)	0.0069(9)
B2	0.4986(9)	0.1391(4)	0.1809(2)	0.0053(11)
B3	0.4980(10)	0.3893(3)	0.0707(3)	0.0057(9)
B4	0.9977(9)	0.1369(4)	0.1789(2)	0.0049(11)

[a] All atoms are located at 8*i* Wyckoff positions with a site occupancy of 1.0. [b] $U_{eq} = (\sum_i \sum_j U_{ij} a_i^* a_j^* \boldsymbol{a}_i \cdot \boldsymbol{a}_j)/3$.

Table 3. Anisotropic Displacement Parameters (U_{ij}) for $Mg_5SnB_2O_{10}$

	Anisotropic Displacement Parameters, U_{ij} (Å^2)					
atom	U_{11}	U_{22}	U_{33}	U_{12}	U_{13}	U_{23}
Sn1	0.0040(2)	0.0037(3)	0.0033(2)	−0.00035(18)	0.00040(19)	0.00036(15)
Sn2	0.0037(2)	0.0030(3)	0.0043(2)	0.00021(19)	0.00011(19)	0.00065(18)
Mg1	0.0069(11)	0.0050(13)	0.0067(10)	−0.0026(9)	0.0010(8)	0.0032(9)
Mg2	0.0036(11)	0.0065(13)	0.0054(10)	0.0008(11)	−0.0011(8)	0.0034(9)
Mg3	0.0064(9)	0.0068(12)	0.0071(9)	−0.0028(9)	0.0007(7)	−0.0004(10)
Mg4	0.0063(9)	0.0054(11)	0.0027(8)	−0.0030(8)	0.0001(7)	0.0018(9)
Mg5	0.0059(7)	0.0057(8)	0.0042(7)	−0.0010(7)	0.0005(6)	0.0017(7)
Mg6	0.0080(8)	0.0064(8)	0.0055(8)	−0.0023(7)	0.0001(6)	−0.0005(8)
Mg7	0.0092(8)	0.0060(8)	0.0049(7)	−0.0002(7)	0.0005(6)	−0.0003(7)
Mg8	0.0033(7)	0.0066(8)	0.0046(7)	−0.0012(7)	0.0046(7)	0.0019(7)
Mg9	0.0066(8)	0.0056(8)	0.0058(8)	0.0000(6)	0.0003(7)	0.0009(6)
Mg10	0.0051(8)	0.0071(8)	0.0047(8)	−0.0003(6)	0.0003(7)	−0.0017(6)

Experimental Section

A. Synthesis of Samples. Polycrystalline $Mg_5Sn_{1-x}Ti_xB_2O_{10}$ solid solutions were synthesized via solid-state reaction. Starting powders of MgO (99.9%, Rare Metallic), SnO_2 (99.9%, Sigma−Aldrich), TiO_2 (99.9%, Rare Metallic), and H_3BO_3 (99.99%, Sigma−Aldrich) were weighed, with $MgO:SnO_2:TiO_2:H_3BO_3$ molar ratios of $= 5:(1 - x):x:2.2$ (where $x = 0$, 0.05, 0.10, 0.20, 0.30, and 0.50). Excess 10 mol % of H_3BO_3 was added to the starting mixtures, in consideration of the volatilization loss of B_2O_3 during heating. The powders were mixed in an agate mortar with a pestle, pressed into pellets, and placed on a platinum plate. The pellets were first heated at 1100 °C for 6 h in air. They were then crushed and pelletized and finally heated at 1300 °C for 24−36 h in air.

Single crystals of $Mg_5SnB_2O_{10}$ were prepared using B_2O_3 as a flux. Approximately 80 mg (0.19 mmol) of the polycrystalline $Mg_5SnB_2O_{10}$ powders and 100 mg (0.81 mmol) of H_3BO_3 were weighed and placed in a platinum boat. The mixture was heated at 1350 °C for 12 h. It was then cooled to room temperature at a rate of ∼15 °C/min.

B. Characterization. Electron diffraction patterns were taken using a transmission electron microscope (JEOL, Model JEM-2000EX, with a beam accelerating voltage of 200 kV), to check the unit-cell dimensions and the crystal lattice of $Mg_5SnB_2O_{10}$.

Table 4. Selected Bond Lengths (Å) and Bond Valence Sums (BVS) for $Mg_5SnB_2O_{10}$

Sn1−O13	1.986(4)	Sn2−O17^{ii}	1.992(4)	Mg1−O18	2.000(4)
Sn1−O14	2.006(3)	Sn2−O18	2.007(4)	Mg1−O17^{iv}	2.025(4)
Sn1−O15	2.066(3)	Sn2−O20	2.061(4)	Mg1−O7	2.089(4)
Sn1−O16	2.069(3)	Sn2−O19^{ii}	2.069(3)	Mg1−O4	2.175(4)
Sn1−O6	2.114(3)	Sn2−O12	2.116(3)	Mg1−O20	2.192(4)
Sn1−O2^{i}	2.145(4)	Sn2−O3^{iii}	2.121(3)	Mg1−O19^{iv}	2.196(4)
BVS[a]	3.94	BVS[a]	3.97	BVS[a]	1.97
Mg2−O14^{v}	2.016(4)	Mg3−O14^{vii}	2.017(4)	Mg4−O17	2.018(4)
Mg2−O13	2.031(4)	Mg3−O13^{viii}	2.021(4)	Mg4−O18	2.018(4)
Mg2−O10^{v}	2.079(4)	Mg3−O9^{iv}	2.071(4)	Mg4−O4^{iv}	2.099(4)
Mg2−O9^{vi}	2.164(4)	Mg3−O9^{ix}	2.096(4)	Mg4−O4	2.119(4)
Mg2−O16	2.171(4)	Mg3−O2^{ix}	2.179(4)	Mg4−O12	2.187(4)
Mg2−O15^{v}	2.180(4)	Mg3−O2^{ii}	2.190(4)	Mg4−O12^{ii}	2.203(4)
BVS[a]	1.99	BVS[a]	2.06	BVS[a]	2.00
Mg5−O13	1.957(4)	Mg6−O17	1.954(4)	Mg7−O18	1.951(4)
Mg5−O19^{x}	2.063(4)	Mg6−O15	2.059(4)	Mg7−O16^{iv}	2.061(4)
Mg5−O11	2.116(4)	Mg6−O1	2.112(4)	Mg7−O1^{ii}	2.114(4)
Mg5−O7^{xi}	2.132(4)	Mg6−O8	2.144(4)	Mg7−O6^{iv}	2.152(4)
Mg5−O5	2.169(4)	Mg6−O10	2.150(4)	Mg7−O8^{iv}	2.155(4)
Mg5−O3^{xi}	2.218(4)	Mg6−O6	2.167(4)	Mg7−O10^{ii}	2.163(4)
BVS[a]	2.00	BVS[a]	2.02	BVS[a]	2.04
Mg8−O14	1.955(4)	Mg9−O16^{vi}	2.086(3)	Mg10−O19^{iv}	2.086(4)
Mg8−O20^{vii}	2.065(4)	Mg9−O15^{i}	2.093(3)	Mg10−O5	2.087(4)
Mg8−O7^{vii}	2.113(4)	Mg9−O8	2.094(4)	Mg10−O20	2.093(4)
Mg8−O11^{iii}	2.119(4)	Mg9−O15	2.109(4)	Mg10−O19^{x}	2.104(4)
Mg8−O5	2.166(4)	Mg9−O16	2.112(4)	Mg10−O20^{vii}	2.104(4)
Mg8−O3^{xi}	2.221(4)	Mg9−O1^{i}	2.185(4)	Mg10−O11^{xi}	2.160(4)
BVS[a]	2.02	BVS[a]	1.94	BVS[a]	1.97
B1−O1	1.361(7)	B2−O4	1.353(7)	B3−O7^{iv}	1.380(7)
B1−O2	1.402(7)	B2−O5	1.387(8)	B3−O8	1.383(7)
B1−O3^{iv}	1.402(8)	B2−O6	1.407(7)	B3−O9	1.401(6)
BVS[a]	2.87	BVS[a]	2.92	BVS[a]	2.86
B4−O10	1.377(7)				
B4−O11^{v}	1.382(7)				
B4−O12	1.400(6)				
BVS[a]	2.88				

Symmetry codes: (i) $-x+{}^{3}/_{2}, -y+{}^{1}/_{2}, -z$; (ii) $-x+2, -y+{}^{1}/_{2}, -z+{}^{1}/_{2}$; (iii) $x+1, y, z$; (iv) $-x+1, -y+{}^{1}/_{2}, -z+{}^{1}/_{2}$; (v) $x-1, y, z$; (vi) $-x+{}^{1}/_{2}, -y+{}^{1}/_{2}, -z$; (vii) $-x+{}^{3}/_{2}, -y, -z+{}^{1}/_{2}$; (viii) $x+{}^{1}/_{2}, y, z+{}^{1}/_{2}$; (ix) $x, y-{}^{1}/_{2}, z+{}^{1}/_{2}$; (x) $x-{}^{1}/_{2}, y-{}^{1}/_{2}, z$; (xi) $-x+{}^{1}/_{2}, -y, -z+{}^{1}/_{2}$. [a] BVS is defined as follows: $V_j = \sum_i \exp[(l_0 - l_{ij})/B]$, where l_0 the bond valence parameters (BVP) presented by Brese and O'Keefe[38] for B−O, Mg−O and Sn−O, l_{ij} is the distance between i and j atoms, and B is a constant value of 0.37 Å. The BVP values of the B^{3+}, Mg^{2+}, and Sn^{4+} ions are 1.371, 1.693, and 1.905 Å, respectively.

XRD data of an $Mg_5SnB_2O_{10}$ single crystal were collected using Mo Kα radiation with a graphite monochromator and an imaging plate on a single-crystal X-ray diffractometer (Rigaku, Model R-AXIS RAPID-II). Diffraction-data collection and unit-cell refinement were performed by the PROCESS-AUTO program.[29] Absorption correction was performed by the NUMABS program.[30]

The crystal structure was solved via a direct method, using the SIR2004 program,[31] and refined by the full-matrix least-squares on F^2, using the SHELXL-97 program.[32] All calculations were carried out on a personal computer, using the WinGX software package.[33] The atomic coordinates were standardized by the STRUCTURE TIDY program.[34]

The pellet samples of $Mg_5Sn_{1-x}Ti_xB_2O_{10}$ were powdered and characterized by powder XRD, using Cu Kα radiation with a graphite monochromator mounted on a powder diffractometer (Rigaku, Model RINT2000). The crystal structure parameters of the solid solutions were refined using the RIETAN-FP program.[35] The crystal structures were illustrated by the VESTA program.[36]

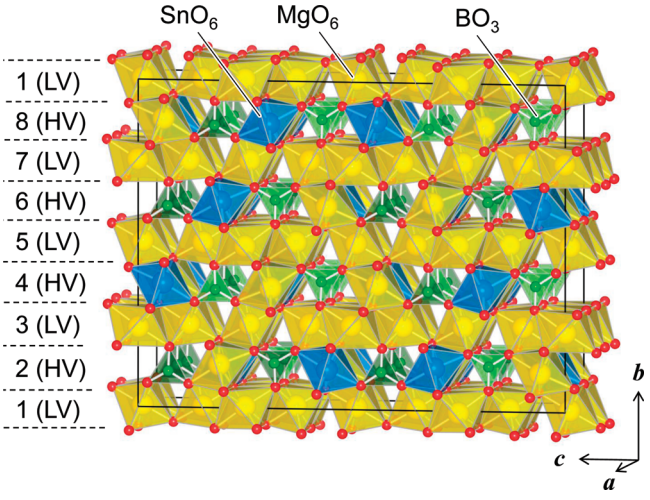

Figure 2. Crystal structure of $Mg_5SnB_2O_{10}$.

(29) PROCESS-AUTO; Rigaku/MSC & Rigaku Corporation: The Woodlands, TX, USA and Akishima, Tokyo, Japan, 2005.
(30) Higashi, T. NUMABS−Numerical Absorption Correction; Rigaku Corporation: Tokyo, 1999.
(31) Burla, M. C.; Caliandro, R.; Camalli, M.; Carrozzini, B.; Cascarano, G. L.; De Caro, L.; Giacovazzo, C.; Polidori, G.; Spagna, R. *J. Appl. Crystallogr.* **2005**, *38*, 381–388.
(32) Sheldrick, G. M. *Acta Crystallogr., Sect. A: Found. Crystallogr.* **2008**, *64*, 112–122.
(33) Farrugia, L. J. *J. Appl. Crystallogr.* **1999**, *32*, 837–838.
(34) Gelato, L. M.; Parthé, E. *J. Appl. Crystallogr.* **1987**, *20*, 139–143.

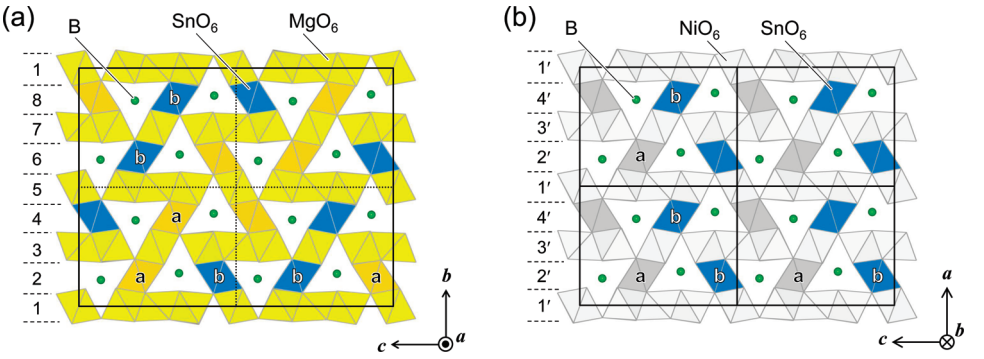

Figure 3. Graphics showing the arrangement of the metal atom-centered octahedra projected (a) on the *bc*-plane for $Mg_5SnB_2O_{10}$ and (b) on the *ac*-plane for $Ni_5SnB_2O_{10}$.

The photoluminescence (PL) excitation and emission spectra of the solid solutions were measured at room temperature with a fluorescence spectrophotometer (Hitachi, F-4500) equipped with a 150-W xenon lamp as an excitation source. The quantum efficiencies of the solid solutions were measured at room temperature using a quantum efficiency measurement system (Otsuka Electronics, Model QE-1000).

Results and Discussion

A. Crystal Structure of $Mg_5SnB_2O_{10}$. The results of the data collection and structure refinements for $Mg_5SnB_2O_{10}$ are listed in Table 1. Observed X-ray and electron diffraction reflections were indexed with the triclinic space group $P\bar{1}$, but we chose the face-centered setting in the space group $F\bar{1}$, with unit-cell parameters of $a = 6.1295(8)$ Å, $b = 18.714(3)$ Å, $c = 24.719(3)$ Å, $\alpha = 90.021(5)°$, $\beta = 90.032(4)°$, and $\gamma = 90.041(5)°$, to analyze and describe the crystal structure and twinning, for comparsion with the basic unit of the orthorhombic ludwigite-type structure. Figure 1 shows an electron diffraction pattern of $Mg_5SnB_2O_{10}$ taken with the incident electron beam parallel to the *a*-axis. Spots split along the *b*-axis suggested the presence of twins in the crystals. The twin matrix of $\boldsymbol{M} = [1\,0\,0, 0\,-1\,0, 0\,0\,1]$ was used in the structure refinement of the twinned crystal. Residual indices for all data were $R1 = 0.0168$, $wR2 = 0.0459$, and $S = 1.297$, which constitute less than a tenth of the *R*-values without consideration of the twin structure. The fractions of the twin domains estimated from the refined BASF parameter were ~0.6 and 0.4.

Atomic coordinates, anisotropic displacement parameters, and selected bond lengths for $Mg_5SnB_2O_{10}$ are listed in Tables 2, 3, and 4. The crystal structure is shown in Figure 2. Mg, Sn, B, and O atoms located at 8*i* Wyckoff positions have 10, 2, 4, and 20 sites, respectively. Mg and Sn atoms are coordinated by six O atoms to form MO_6 (M = Mg and Sn) octahedra. Each octahedron is connected by sharing via the edges, and zigzag walls infinitely run along the *a*-axis. B atoms are coordinated by three O atoms to form isolated borate groups of BO_3. The bond

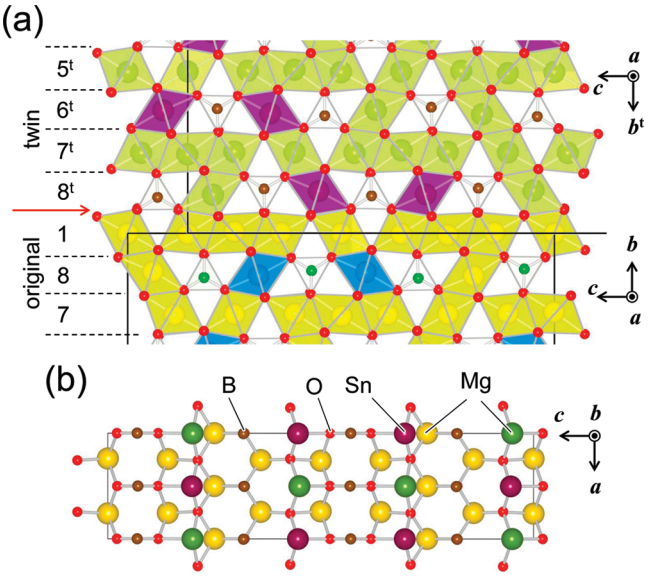

Figure 4. Schematic illustrations of (a) an orthopinakiolite-type zigzag wall introduced by twinning and (b) an atomic arrangement at the twin boundary. A "t" superscript is added to the layer labels of the twin domain.

valence sum (BVS)[37,38] values shown in Table 4 were calculated to be ~2, ~4, and ~3 for Mg, Sn, and B atoms, respectively, and these values agreed well with the formal charges of the elements.

The type of zigzag walls observed in $Mg_5SnB_2O_{10}$ does not appear in orthopinakiolite ($Mg_3Mn_3B_2O_{10}$), but it does in ludwigite (Mg_2FeBO_5). In Figure 2, the crystal structure is divided into eight layers, perpendicular to the *b*-axis. The odd-numbered layers (composed of MgO_6) and the even-numbered layers (composed of MgO_6, SnO_6, and BO_3) are termed the low-valence (LV) and high-valence (HV) layers, respectively.[39] The arrangement of the metal atom centered oxygen octahedra projected on the *bc*-plane for $Mg_5SnB_2O_{10}$ and the *ac*-plane for $Ni_5SnB_2O_{10}$[27] are shown in Figure 3. The $M^{II}O_6$ (where M^{II} = Mg or Ni) octahedra and SnO_6 octahedron are labeled a and b, respectively. The alternate arrangements of the Mg and Sn atoms along the *a*-axis of $Mg_5SnB_2O_{10}$ are the same as those of the Ni and Sn atoms

(35) Izumi, F.; Momma, K. *Solid State Phenom.* **2007**, *130*, 15–20.
(36) Momma, K.; Izumi, F. *J. Appl. Crystallogr.* **2008**, *41*, 653–658.
(37) Brown, I. D.; Altermatt, D. *Acta Crystallogr., Sect. B: Struct. Sci.* **1985**, *41*, 244–247.
(38) Brese, N. E.; O'Keeffe, M. *Acta Crystallogr., Sect. B: Struct. Sci.* **1991**, *47*, 192–197.
(39) Takéuchi, Y. *Tropochemical Cell-Twinning*; Terra Scientific Publishing Company; Tokyo, 1997; pp 113−159.

Table 5. Results of the Rietveld Analysis and Crystal Structure Data for $Mg_5Sn_{1-x}Ti_xB_2O_{10}$ (x = 0 and 0.50)

parameter	Value	
	$x = 0$	$x = 0.50$
crystal system	triclinic	triclinic
space group	$P\bar{1}$ (No. 2)	$P\bar{1}$ (No. 2)
unit-cell dimensions		
a	6.12440(11) Å	6.07328(12) Å
b	9.84386(14) Å	9.79279(17) Å
c	12.73827(15) Å	12.69900(17) Å
α	85.733(2)°	85.7201(16)°
β	76.1369(16)°	76.113(2)°
γ	71.9101(18)°	71.887(2)°
unit-cell volume, V	708.7(5) Å^3	696.9(6) Å^3
Z	2	2
2θ range	5°−140°	5°−140°
R indices		
R_{wp}	0.10302	0.09216
R_p	0.07461	0.06763
R_B	0.02183	0.02142
R_F	0.01239	0.01231
goodness-of-fit, S	1.7811	1.5217
site occupancy factors, g		
g(Sn1/Ti1)	1/0	0.5/0.5
g(Sn2/Ti2)	1/0	0.5/0.5
Sn1/Ti1−O, Sn2/Ti2−O bond lengths		
l_{short}	2.00(6) Å, 1.98(7) Å	1.91(4) Å, 1.89(5) Å
l_{long}	2.22(3) Å, 2.17(3) Å	2.15(4) Å, 2.14(3) Å
l_{av}	2.08(6) Å, 2.08(5) Å	2.04(4) Å, 2.05(4) Å
(Sn/Ti)O$_6$-octahedral volumes, V_{oct}		
(Sn1/Ti1)O$_6$	11.7 Å^3	11.1 Å^3
(Sn2/Ti2)O$_6$	11.8 Å^3	11.3 Å^3

along the b-axis of $Ni_5SnB_2O_{10}$. The a and b octahedra are arranged in the order of

$$\cdots - a - b - b - a - \cdots$$

along the b- and c-axes of $Mg_5SnB_2O_{10}$ (see Figure 3a), while the a and b octahedra are arranged in the order of

$$\cdots - a - b - a - b - \cdots$$

along the a- and c-axes of $Ni_5SnB_2O_{10}$ (see Figure 3b). $Mg_5SnB_2O_{10}$ (a = 6.1295(8) Å, b = 18.714(3) Å, and c = 24.719(3) Å) has a novel superstructure in which the b- and c-axis lengths are approximately two times the a- and c-axis lengths of $Ni_5M^{IV}B_2O_{10}$ (M^{IV} = Sn and Hf; $a \approx 9$ Å, $b \approx 6$ Å, and $c \approx 12$ Å).[27,28]

Bovin et al. investigated the crystal structures of mineral and synthetic M_3BO_5-type oxyborates by high-resolution transmission electron microscopy and observed defect structures in orthopinakiolite and pinakiolite but not in ludwigite.[40,41] Cooper and Tilley reported that the orthopinakiolite-type structure was partially derived from planar defects in the crystal structure of $Mg_{1.5}Mn_{1.5}BO_5$ with the ludwigite-type structure.[42] The planar defects are twin planes in the layers. According to these twin structures, we present a twinned model for $Mg_5SnB_2O_{10}$. Figure 4 shows the twin domain drawn by inverting the y-coordinates

(40) Bovin, J. -O.; O'Keefe, M.; O'Keefe, M. A. *Acta Crystallogr., Sect. A: Found. Crystallogr.* **1981**, *37*, 28–35.
(41) Bovin, J. -O.; O'Keefe, M. *Acta Crystallogr., Sect. A: Found. Crystallogr.* **1981**, *37*, 35–42.
(42) Cooper, J. J.; Tilley, R. J. D. *J. Solid State Chem.* **1985**, *58*, 375–382.

Table 6. Atomic Coordinates and Isotropic Atomic Displacement Parameters (B) for $Mg_5Sn_{0.50}Ti_{0.50}B_2O_{10}$ with the $P\bar{1}$ Cell[a]

atom	occ.	x	y	z	B (Å)
Sn1/Ti1	0.5/0.5	0.3180(15)	0.2415(6)	0.1160(7)	0.50(2)
Sn2/Ti2	0.5/0.5	0.5576(17)	0.2619(9)	0.6152(6)	0.50[b]
Mg1	1	0.057(6)	0.261(3)	0.616(2)	0.50[b]
Mg2	1	0.822(5)	0.2384(19)	0.1144(19)	0.50[b]
Mg3	1	0.251(3)	−0.001(6)	0.999(3)	0.50[b]
Mg4	1	0.232(3)	0.498(5)	0.499(3)	0.50[b]
Mg5	1	0.095(4)	0.003(4)	0.280(2)	0.50[b]
Mg6	1	0.390(4)	0.502(4)	0.216(3)	0.50[b]
Mg7	1	0.098(4)	0.496(4)	0.784(3)	0.50[b]
Mg8	1	0.605(4)	0.004(5)	0.281(3)	0.50[b]
Mg9	1	0.234(5)	0.5106(9)	0.0009(7)	0.50[b]
Mg10	1	0.267(4)	0.006(1)	0.4989(8)	0.50[b]
O1	1	0.641(6)	0.620(3)	0.144(2)	0.284[c]
O2	1	0.543(8)	0.842(4)	0.045(3)	0.529[c]
O3	1	0.545(8)	0.158(4)	0.7683(19)	0.490[c]
O4	1	0.108(8)	0.351(4)	0.456(2)	0.387[c]
O5	1	0.258(9)	0.123(4)	0.354(2)	0.758[c]
O6	1	0.203(8)	0.352(3)	0.2616(18)	0.316[c]
O7	1	0.063(6)	0.144(3)	0.7719(17)	0.521[c]
O8	1	0.129(7)	0.631(3)	0.146(2)	0.363[c]
O9	1	0.025(5)	0.850(4)	0.037(2)	0.426[c]
O10	1	0.722(6)	0.351(3)	0.2569(17)	0.505[c]
O11	1	0.737(8)	0.134(4)	0.358(2)	0.521[c]
O12	1	0.605(8)	0.353(4)	0.456(2)	0.521[c]
O13	1	0.243(7)	0.389(7)	0.643(5)	0.450[c]
O14	1	0.154(5)	0.100(5)	0.143(4)	0.284[c]
O15	1	0.629(6)	0.103(6)	0.145(4)	0.426[c]
O16	1	0.254(7)	0.609(7)	0.358(5)	0.418[c]
O17	1	0.110(6)	0.882(7)	0.428(5)	0.474[c]
O18	1	0.535(6)	0.384(6)	0.082(4)	0.418[c]
O19	1	0.413(6)	0.116(7)	0.573(5)	0.434[c]
O20	1	0.049(5)	0.383(5)	0.081(4)	0.521[c]
B1	1	0.547(16)	0.784(4)	0.135(5)	0.545[c]
B2	1	0.171(13)	0.273(5)	0.362(3)	0.418[c]
B3	1	0.044(15)	0.785(4)	0.137(6)	0.450[c]
B4	1	0.675(11)	0.258(4)	0.352(3)	0.387[c]

[a] All atoms are located at 2i Wyckoff positions. [b] The values were fixed with B(Sn1/Ti1). [c] The values were fixed with those of the $Mg_5SnB_2O_{10}$ single crystal.

of the original atomic coordinates. The twin boundary is indicated by the arrow in the figure. Instead of the 2 layer of the original domain, the 8^t layer of the twin domain is stacked next to the 1 layer of the original domain in this model. The crystal structure is then partially transformed from the ludwigite-type structure to the orthopinakiolite-type structure. Figure 4b shows an arrangement of atoms in proximity to the twin boundary. The 1 and 8^t layers are able to be stacked without a large mismatch via O atoms at the twin boundary.

B. $Mg_5Sn_xTi_{1-x}B_2O_{10}$ Solid Solutions. The atomic coordinates of $Mg_5SnB_2O_{10}$ with the $F\bar{1}$ cell shown in Table 2 were transformed to those with the $P\bar{1}$ cell for the Rietveld analysis of the powder XRD patterns of the solid solutions. The transform matrices between space groups the $F\bar{1}$ and $P\bar{1}$ are $\boldsymbol{R}_{F\rightarrow P}$ = [1 0 0, 0.5 0.5 0, 0.5 0 0.5] and $\boldsymbol{R}_{P\rightarrow F}$ = [1 0 0, −1 2 0, −1 0 2]. The refinement results of $Mg_5Sn_xTi_{1-x}B_2O_{10}$ (x = 0 and 0.50) and the refined atomic coordinates of $Mg_5Sn_{0.50}Ti_{0.50}B_2O_{10}$ are listed in Tables 5 and 6, respectively. The site occupancy factors (g) at the Sn/Ti sites were fixed with the nominal mixing ratios of the starting materials. The Rietveld refinement plots of $Mg_5Sn_xTi_{1-x}B_2O_{10}$ (x = 0 and 0.50) are shown in Figure 5. All reflections observed from the solid solutions with the

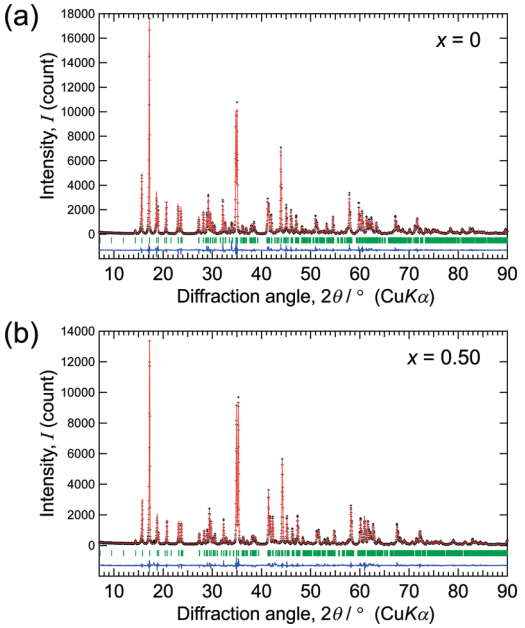

Figure 5. Rietveld plots of $Mg_5Sn_{1-x}Ti_xB_2O_{10}$ with compositions of (a) $x = 0$ and (b) $x = 0.50$. The vertical lines represent the diffraction angles of all possible Bragg reflections.

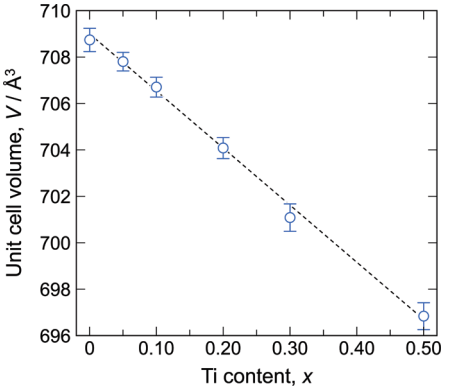

Figure 6. Unit-cell volume of the $Mg_5Sn_{1-x}Ti_xB_2O_{10}$ solid solutions, as a function of the titanium content (x).

composition of $x = 0-0.50$ were indexed with the triclinic unit-cell parameters of $Mg_5Sn_{1-x}Ti_xB_2O_{10}$. As shown in Figure 6, the unit-cell volumes (V) of the solid solutions decreased as the titanium content (x) increased.

The PL excitation and emission spectra of $Mg_5Sn_{0.90}Ti_{0.10}B_2O_{10}$ are shown in Figure 7, along with those reported by Konijnendijk and Blasse.[11] An absorption band attributed to the CT transition in TiO_6 octahedra was observed in the wavelength range of 220−320 nm. The excitation peak wavelengths of $Mg_5Sn_xTi_{1-x}B_2O_{10}$ (x = 0.05−0.50) shifted from 260 nm to 270 nm with increasing x from 0.05 to 0.50. The shape and the peak position in the excitation spectra were sharper and longer than those reported in the previous study.[11] The solid solutions, except for the host compound of $Mg_5SnB_2O_{10}$, showed a broad blue emission with peak wavelengths of ~430 nm. Changes of the spectrum shape and peak position due to increasing titanium contents were scarcely observed in the emission spectra measured in the present study. The relative emission intensities at 430 nm are plotted against the titanium content

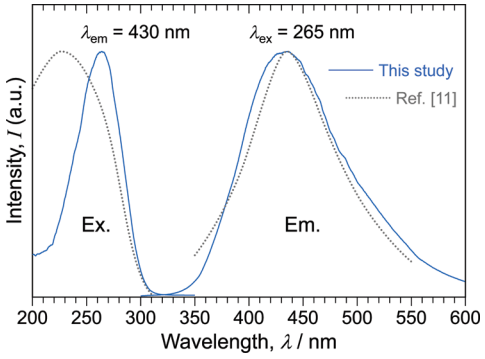

Figure 7. Photoluminescence excitation and emission spectra of $Mg_5Sn_{0.90}Ti_{0.10}B_2O_{10}$, along with those reported by Konijnendijk and Blasse.[11]

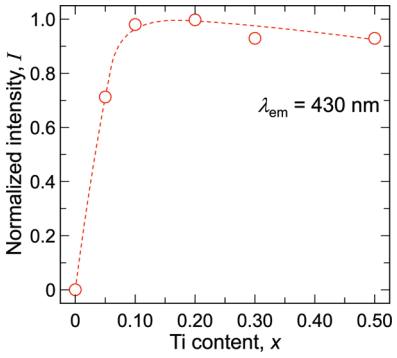

Figure 8. Relative emission intensity as a function of the titanium content (x).

in Figure 8. $Mg_5Sn_{0.80}Ti_{0.20}B_2O_{10}$ showed the maximum emission intensity, and a quantum efficiency of 0.81 was measured at room temperature.

In this solid solution series, significant concentration quenching of the luminescence did not occur. Blasse studied concentration quenching of the luminescence of Ti^{4+} complexes[4] and concluded that concentration quenching could be reduced if TiO_n polyhedra involving the luminescence separate from neighboring polyhedra in the host compounds. In the crystal structure of $Mg_5SnB_2O_{10}$, which was first determined by the crystal structure analysis in the present study, the substituent Ti atoms inevitably form isolated TiO_6 octahedra, because of the ordered arrangement of MgO_6 and SnO_6 octahedra. The shortest distance between the Sn/Ti sites clarified by the present study is ~5.3 Å. Therefore, excitation energy could be efficiently converted to emission energy without energy transfer from the excited Ti^{4+} ions to the neighboring Ti^{4+} ions in the solid solutions, even with a high titanium content of $x = 0.50$. A similar result was reported for $BaSn_{1-x}Ti_xSi_3O_9$ solid solutions. The TiO_6 octahedra are separated by Ba atoms and Si_3O_9 groups in the host compound of $BaSnSi_3O_9$,[9] and the shortest distance between the Sn/Ti sites is ~4.9 Å. Forming isolated TiO_n polyhedra in host compounds would have an effect on repression of the concentration quenching of Ti^{4+}-activated phosphors.

Summary

Single crystals of $Mg_5SnB_2O_{10}$ ($Mg_5Sn(BO_3)_2O_4$) were synthesized using B_2O_3 as a flux at 1350 °C in air. The crystal structure was analyzed by single-crystal X-ray diffraction.

$Mg_5SnB_2O_{10}$ crystallizes in the triclinic space group $F\bar{1}$ (No. 2) and was found to have a novel ludwigite-related superstructure with an ordered distribution of Mg and Sn atoms. Titanium(IV)-doped solid solutions of $Mg_5Sn_{1-x}Ti_xB_2O_{10}$ ($0 < x \leq 0.50$) prepared at 1300 °C in air showed a broad blue emission with a peak wavelength at 430 nm under 265 nm excitation. The maximum emission intensity was observed for $Mg_5Sn_{0.80}Ti_{0.20}B_2O_{10}$, with a quantum efficiency of 0.81 at room temperature. Significant concentration quenching did not occur in this solid-solution series.

Acknowledgment. This work was supported in part by the Global COE Program "Materials Integration, Tohoku University" and by a Grant-in-Aid for Scientific Research (B) (No. 21350113, 2009) from the Ministry of Education, Culture, Sports and Technology (MEXT), Japan.

Supporting Information Available: Crystal information file and list of structure factors for $Mg_5SnB_2O_{10}$, and the results of Rietveld refinement for the $Mg_5Sn_xTi_{1-x}B_2O_{10}$ solid solutions. This material is available free of charge via the Internet at http://pubs.acs.org.